Structures and Photoelectron Spectroscopies of $Si_2C_2^-$ Studied with ab Initio Multicanonical Monte Carlo Simulation

Pradipta Bandyopadhyay,[†] Seiichiro Ten-no, and Suehiro Iwata*

Graduate University for Advanced Studies and Institute for Molecular Science, Okazaki 444-8585, Japan

Received: March 24, 1999; In Final Form: June 14, 1999

Experimental photoelectron spectrum of $Si_2C_2^-$ was assigned by ab initio Monte Carlo simulation with the multicanonical/histogram reweighting technique. At first, two structures, linear and ring, were optimized at the MP2/6-31G* level. The multireference configuration interaction (MRCI) calculation reveals that the spectrum cannot be assigned by considering only a single isomer. Also, MRCI calculations cannot explain different widths of the peaks in the spectrum. Multicanonical Monte Carlo simulation with configuration interaction calculation at each step of the simulation was performed for both ring and linear isomers to include the effects of large nuclear motion at finite temperature on the spectrum. It was found that a mixture of two isomers at the experimental condition is necessary to assign the spectrum.

1. Introduction

Investigations of mixed silicon−carbon clusters are challenging because of the complexity associated with structures and spectroscopies of these clusters. Also, from the point of view of application, they are important in silicon carbide industry. In addition, a few Si_nC_m molecules have been detected in the interstellar space, which has triggered more systematic spectroscopic studies. These clusters are subjects of numerous recent theoretical and experimental studies.[1−4] The complexity in the structures of them comes from the inherent differences in the bonding abilities of carbon and silicon. Carbon can form multiple bonds easily, as is exemplified by the diversity of structures in organic chemistry, whereas silicon prefers single bonds. This different bonding ability is also seen in the structural differences of pure silicon and carbon clusters. From ab initio MO calculations,[5] it was found that, in even-numbered C_n clusters ($n = 4, 6, 8, 10$), ring structures of the singlet state are the lowest in energy and a linear isomer of the triplet state lies close to it. Odd-numbered C_n clusters ($n = 3, 5, 7, 9$) prefer linear structures of the singlet state. On the other hand, Si_n clusters[6] prefer cagelike structures for $5 \leq n \leq 11$. Obviously, in mixed clusters, structures are difficult to predict intuitively. They might have several isomers within a small energy range, depending upon the numbers of silicons and carbons.

Several recent studies[7,8] have investigated structures and spectra of mixed clusters. From the theoretical side, the main emphasis has been use of density functional theory to probe structures of the clusters. Experimentally photoelectron and infrared spectroscopy have been extremely useful in probing the structures. A recent theoretical study by Hunsicker and Jones[2] combined density functional calculation with molecular dynamics to find the various isomers of neutral and anionic mixed cluster.

Statistical mechanical simulation techniques are promising for investigating the complex potential energy surfaces of the mixed clusters. Since there is yet to be any reliable potential energy functions for these systems, ab initio simulation might be the only way for treating these systems. Statistical mechanical treatment allows investigation of the finite temperature effects on the structure and spectroscopy. Indeed, in the experiment of mixed clusters by Nakajima et al.,[3] several complex spectra were attributed to the presence of different isomers at the experimental condition. The most complex spectrum in their experiment was for $Si_2C_2^-$, which showed at least four peaks and the origin of which could not be assigned properly. In the present work, we focused our attention on the structure and assignment of the photoelectron spectrum of $Si_2C_2^-$ by combining ab initio molecular orbital theory with the multicanonical Monte Carlo simulation. To find the finite temperature effect on the spectrum and structure, we performed multicanonical Monte Carlo (MC) simulation with a small configuration interaction calculation at each step of the simulation. From the simulation, we proposed the average structure of $Si_2C_2^-$ at finite temperature and assigned the spectrum on the basis of the proposed structures. To estimate the relative energy between the isomers and the photodetachment energy, a high level of electronic structure calculations with a large basis set is required. Using the high-level calculations, the MC results of low-level ab initio calculations were properly calibrated.

This paper is organized in the following way. In section 2, we describe the computational details of the ab initio calculation. Section 3 consists of the assignment of the spectrum on the basis of multireference configuration interaction calculations. In section 4, the multicanonical algorithm is described. In section 5, the average structure of $Si_2C_2^-$ and the assignment of the spectrum are given from the results of the simulation. The paper ends with a conclusion in section 6.

2. Details of ab Initio MO Calculation

The geometrical structure, electronic structure, and photoelectron spectrum of $Si_2C_2^-$ were studied by high-level ab initio molecular orbital (MO) theory and by a novel combination of MO calculation and multicanonical Monte Carlo (MC) simulation. The various photodetached states of Si_2C_2 and the ground state of $Si_2C_2^-$ were studied at a highly correlated ab initio method to estimate the vertical detachment energies (VDEs).

[†] Present address: Department of Chemistry, Iowa State University, IA, 50011.

* Corresponding author. E-mail: iwata@ims.ac.

10.1021/jp991004x CCC: $18.00
Published on Web 07/23/1999

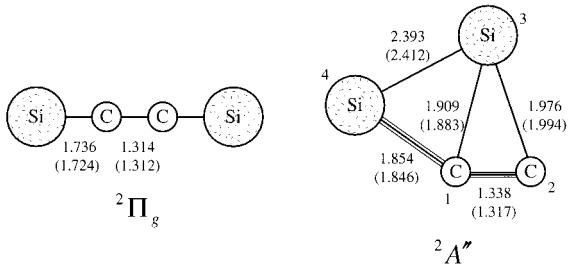

Figure 1. Two minimum structures of $Si_2C_2^-$ optimized at the MP2/6-31+G* level. The numbers 1−4 represent atom numbers. The bond lengths are also given. The numbers in parentheses denote the values obtained by Hunsicker and Jones (ref 2). Bond lengths are given in angstroms.

2.A. Ab Initio Molecular Orbital Calculation. The structures of $Si_2C_2^-$ were optimized at the ROHF/MP2 level of theory with the 6-31+G* basis set. In agreement with the previous study,[2] we found two structures which are at the minima on the potential energy surface. One is linear with two silicon atoms at the ends of the chain, and the other is a distorted trapezoid with C_s symmetry, which in what follows will be described as the ring structure. Relative stability of these two structures is a matter of controversy. Hunsicker and Jones found that the ring one was more stable by 0.1 eV at their density functional calculation with local density approximation. However, in our optimized structures, the linear one is more stable by 0.147 eV. CCSD(T) calculations with the AVTZ basis set on the optimized structures show that the ring structure is slightly more stable by 0.013 eV. The two isomers are shown in Figure 1. The calculation of harmonic frequencies confirms that these two isomers are indeed minima on the potential energy surface. It is to be noted that the D_{2h} structure was found to be a second order saddle point. Special care was taken to eliminate symmetry broken structures, which is often the case with molecules with one odd electron. For the calculation of VDEs, it is known that dynamic correlation effect can contribute as much as 1 eV and only highly correlated wave function methods can recover most of the correlation energy. We performed internally contracted multireference configuration interaction (MRCI) calculation[9] for the accurate evaluation of VDEs for the linear and ring structures. The calculations for ring and linear isomers are described below. All the calculations were performed using MOLPRO,[10] GAMESS,[11] and GAUSSIAN[12] program packages.

2.B. Ring Structure. For the ring structure, MRCI calculations were performed with the natural orbitals obtained from a preceding CASSCF calculation. The basis set used was Dunning's augmented valence double-zeta (AVDZ).[13] The valence electronic configuration can be written by $\Lambda(17a')^2(4a'')^1$, where Λ denotes $(11a')^2(12a')^2(13a')^2(14a')^2(3a'')^2(15a')^2(16a')^2$ occupation. In the CASSCF calculation, the active space consisted of 14a′, 15a′, 16a′, 17a′, 18a′, 19a′, 3a″, 4a″, and 5a″ orbitals. All other occupied orbitals were kept doubly occupied in all the configurations used in the CASSCF calculation. This gives rise to 11 electrons in 9 orbitals for the anion and 10 electrons in 9 orbitals for the neutral species in the active space. In the next step of the calculation, internally contracted MRCI calculations were performed for the anion and neutral (singlet and triplet) with the respective CASSCF reference functions to recover the dynamical part of the correlation energy. The MRCI wave functions were generated by all single and double excitations from the active orbitals of the CASSCF reference. For the neutral system, the singlet and triplet states were calculated separately. The results of this calculation are given in Table 1. The most important configuration for the lowest singlet state is $\Lambda(17a')^2$, and that for the triplet isomer is Λ-$(17a')^1(4a'')^1$. These configurations contribute more than 91% to the CI wave functions for both anion and neutral. At the optimized geometry for the anion, the lowest state of the neutral ring isomer is the singlet state, and the triplet state lies above the singlet state by 0.748 eV. The singlet state of the neutral has been found to be a stationary point in the potential energy surface in a previous calculation.[14] As is given in Table 1, if the ring form is assumed for $Si_2C_2^-$, two bands in the photoelectron spectrum at 1.83 eV due to the singlet state and 2.57 eV due to the triplet state are expected. The odd electron is located mostly at the π orbitals of C(2) and Si(4) (see Figure 1).

TABLE 1: Results of the MRCI Calculation for the Ring and Linear Isomers of $Si_2C_2^-$ with the AVDZ Basis Set

isomer	species	state	VDE/eV (total energy/hartree)[a]
ring	$Si_2C_2^-$	$^2A''$	(−653.76005)
	Si_2C_2	$^1A'$	1.825
	Si_2C_2	$^3A''$	2.573
linear	$Si_2C_2^-$	$^2\Pi$	(−653.82129)
	Si_2C_2	$^3\Sigma_g$	1.726
	Si_2C_2	$^1\Delta_g$	2.024
	Si_2C_2	$^1\Sigma_g^+$	2.235

[a] Total energy is in parentheses with hartree, and the vertical detachment energy (VDE) is in electronvolts.

2.C. Linear Structure. The linear $D_{\infty h}$ structure was calculated in the D_{2h} symmetry. The valence electronic configuration of the linear isomer is given by $(9\sigma_g)^2(9\sigma_u)^2(10\sigma_g)^2(10\sigma_u)^2$-$(11\sigma_g)^2(3\pi_u)^4(3\pi_g)^3$, which transforms in the D_{2h} symmetry as $(5a_g)^2(5b_{1u})^2(6a_g)^2(6b_{1u})^2(7a_g)^2(2b_{2u})^2(2b_{3u})^2(2b_{3g})^2(2b_{2g})^1$. In the CASSCF calculation, 6−8a_g, 2−3b_{3u}, 2−3b_{2u}, 6−7b_{1u}, 2b_{2g}, and 2b_{3g} orbitals were taken as the active space. There were 13 electrons in 11 orbitals for the anion and 12 electrons in 11 orbitals for the neutral species. For the anion, the state-specific CASSCF calculation for the $^2B_{3g}$ state was carried out, whereas for the neutrals, the four-state averaged CASSCF calculation was carried out with two states of ^1A_g symmetry and one state each of $^3B_{1g}$ and $^1B_{1g}$ symmetry. Some preliminary calculations showed that these wave functions can describe the low-lying states of the neutral molecule. As the π^2 configuration of the neutral gives rise to the $^1\Sigma_g^+$ (^1A_g), $^1\Delta_g$ (^1A_g and $^1B_{1g}$), and $^3\Sigma_g^-$ ($^3B_{1g}$) states, we focused our attention on these states. For the anion, the MRCI calculation was performed using the CASSCF reference functions for the anion. For the neutrals, MRCI calculations were carried out with the natural orbitals obtained from the diagonalization of the state-averaged density matrix of the preceding CASSCF calculation for the neutral species. The results of the calculation for the linear $Si_2C_2^-$ are given in Table 1. At the optimized geometry for the linear anion, the $^3\Sigma_g^-$ state is the lowest in energy in the neutral, followed by $^1\Delta_g$ and then $^1\Sigma_g^+$. Thus, if the linear isomer is assumed, the bands in the photoelectron spectrum are expected at 1.73, 2.02, and 2.24 eV.

3. Temporal Assignment of the Spectrum

Calculated MRCI bands superimposed on the experimental photoelectron spectrum of Nakajima et al. are shown in Figure 2. Below 3 eV, theoretical calculations predict two bands for the ring isomers and three bands for the linear isomers. The experimental spectrum has more bands that can come from a single isomer, which suggests the coexistence of both isomers at the experimental condition. However, for quantitative comparison between experiment and theory, it is necessary to have

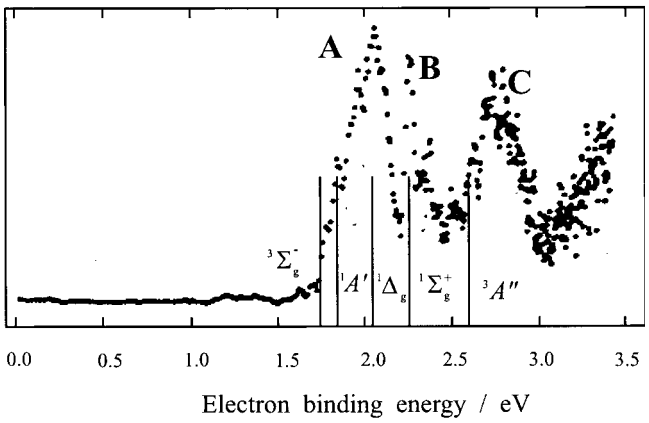

Figure 2. Vertical electron detachment energies evaluated with MRCI calculations, superimposed on the experimental photoelectron spectrum of $Si_2C_2^-$ (ref 3). Labels beside the sticks denote the final states of the detachment.

an estimate of the error bar of our calculations. There are two sources of errors in the calculations, from the basis set and from the quality of many-electron wave functions. As anions are expected to be more stabilized with the sophistication of the wave function, the absolute values of the calculated VDEs are expected to increase. To have some idea of the accuracy of the calculation, MRCI calculation with AVDZ basis was performed for a similar system, Si_3C^-, which has a ring form. From the experiment, the VDE of this molecule has been estimated unambiguously as 1.54 ± 0.08 eV[3]. From our calculation we got the VDE as 1.33 eV. So our calculation underestimates VDE by 0.1−0.3 eV. If it is assumed that the same error holds for $Si_2C_2^-$, the peaks marked A (2.0 eV), B (2.2 eV), and C (2.7 eV) in Figure 2 might be assigned. Peak A may have contribution from the $^3\Sigma_g^+$ state of the linear isomer and $^1A'$ state of the ring structure. While peak B may be contributed by $^1\Delta_g$ and $^1\Sigma_g^+$ states of the linear isomer. Peak C may be from the $^3A''$ state of the ring structure. However, the different widths of the bands cannot be explained by the MRCI calculations.

However, there are two points which need to be discussed. The first one is the relative population of the two isomers at the experimental condition. As the barrier height is expected to be very high for this covalently bonded system, it is safe to assume that there is not much chance of interconversion between the two isomers, once they are produced in the molecular beam. Below, we confirm this assumption in the simulation. Two isomers must have been produced independently by the production mechanism during the experiment. The second point is the relative intensities among the peaks. As the calculation of the matrix element involving the wave function of the detached electron is difficult, the relative intensities among the peaks were not considered quantitatively. We performed multicanonical Monte Carlo simulation separately for the linear and the ring isomers, which should make it possible to find the effect of finite temperature on the structure and spectrum and the appearance and disappearance of some peaks. In the next section, at first the multicanonical algorithm and later the details of the simulation are described.

4. Multicanonical Monte Carlo Simulation

Multicanonical Monte Carlo simulation with histogram reweighting technique was performed to estimate the finite temperature effects on the structures and spectrum of $Si_2C_2^-$. For the electronic structure part, a configuration interaction calculation was performed at each step of the simulation to evaluate the detachment energy. The simulation technique has been described in detail in our previous application.[15] Here, we describe the algorithms very briefly for the sake of completeness. The multicanonical algorithm started as a technique for efficient sampling of the configuration space in the Monte Carlo simulation.[16] In the standard canonical simulation, the probability distribution of a state having energy E is given by

$$P_{\mathrm{can}}(E,\beta) = \frac{n(E)\, \mathrm{e}^{-\beta E}}{\int \mathrm{d}E_s n(E_s)\, \mathrm{e}^{-\beta E_s}}$$

where $n(E)$ is the density of the states and $\beta = 1/k_B T$. In the multicanonical simulation, the probability distribution is made artificially uniform and is given by

$$P_{\mathrm{mu}}(E) = \frac{n(E) W_{\mathrm{mu}}(E)}{\int \mathrm{d}E_s n(E_s) W_{\mathrm{mu}}(E_s)} \approx \text{constant}$$

which implies that the multicanonical weight factor $W_{\mathrm{mu}}(E)$ is independent of temperature and is inversely proportional to the density of states, i.e., $W_{\mathrm{mu}}(E) \propto n(E)^{-1}$. Hence, the multicanonical weight factor is given by $\exp[-S(E)]$, where S is the micorcanonical entropy. Thus, in this algorithm the statistical weight for sampling an energy state is not the Boltzmann factor, but is determined by $\exp[-S(E)]$. The trial entropy function is determined iteratively. It is updated according to the energy histogram from the previous iteration. From this simulation one can not only locate the energy global minimum but also get the canonical distributions for a range of temperature by the histogram reweighting technique.[17] This technique improves the efficiency of the Monte Carlo simulation. It is also possible to calculate the average of any physical quantity A for a wide range of temperature by

$$\langle A \rangle_T = \frac{\int^{\mathrm{mu}} \mathrm{d}x\, A(x) W_{\mathrm{mu}}^{-1}(E(x))\, \mathrm{e}^{-E(x)/k_B T}}{\int^{\mathrm{mu}} \mathrm{d}x\, W_{\mathrm{mu}}^{-1}(E(x))\, \mathrm{e}^{-E(x)/k_B T}}$$

where x stands for a configuration, $E(x)$ is the energy of the configuration x, and $W_{\mathrm{mu}}(E(x))$ is the multicanonical weight factor at configuration x. This has the potential of reducing the computational cost of simulation drastically. However, if the sampling of the states is not good enough, the reweighted averages would be of little value. Combination of multicanonical and reweighting technique alleviates this problem to a considerable extent. This combination is an ideal tool to study the structure and spectra of real molecular systems when combined with ab initio calculations.

4.A. Details of Simulation. It is clear that only a high level of electronic structure calculation with a large basis set can describe the reliable detachment energy for the present system. Also the quasidegeneracy of the neutral singlet state of the linear isomer necessitates multireference treatment. However, use of correlated method with a large basis set is almost prohibited at each step of the Monte Carlo simulation. For this reason, we made a compromise. We used a small basis set, 3-21G*, with effective core potentials (SBK)[18] for both silicon (2s, 2p) and carbon (1s). For every step the restricted open-shell SCF calculation for the anion (which can be described by a single determinant) is followed by a small configuration interaction calculation for the neutral species using the ROHF orbitals of the anion.

The configuration interaction calculation was performed by taking four electrons in three orbitals, two HOMOs and 1

TABLE 2: Energy Differences between Anion and Neutral (Singlet and Triplet) in (4,3) CI and MRCI Calculations for the Optimized Structures at the MP2/6-31+G* Level with *E*(S), *E*(T), and *E*(A) Representing the Energy of the Neutral Singlet, Neutral Triplet, and Anion[a]

	E(S) − *E*(A)		*E*(T) − *E*(A)		*E*(S) − *E*(T)	
	MRCI	(4,3) CI	MRCI	(4,3) CI	MRCI	(4,3) CI
linear	2.024	1.415	1.726	1.122	0.298	0.293
ring	1.825	1.286	2.573	2.225	−0.748	−0.957

[a] All values are given in electronvolts.

SOMO, of the anion. A code was written for this configuration interaction calculation and combined with the program used for simulation. Determinants were constructed for $M_S = 0$ within the active space. This gives rise to nine determinants. Matrix elements between the determinants were evaluated using the Slater−Condon rules. In what follows, this configuration interaction calculation will be denoted as (4,3) CI.

Thus, from each step of the simulation, we can get the singlet−triplet splitting for the neutral species. Despite the severe approximation used, the singlet−triplet separation in the (4,3) CI is reasonably close to the values calculated by the MRCI method (Table 2). In the simulation, one of the four atoms was chosen randomly and the selected atom was given a translational move. The simulation consists of two steps. In the first step, the weight factor for the production run was determined in an iterative way by short simulations starting from a high-temperature canonical simulation. In the next step, a long simulation was carried out with the determined weight factor. After the simulation is complete, canonical distributions for various properties at finite temperatures were determined by the reweighting technique. We carried out two separate simulations for the ring and linear isomers with different weight factors. 30 000 configurations were sampled in the simulation for both the ring and linear isomer. As the difference of energies between the ring and linear isomer is 20 kcal/mol at the ROHF/3-21G* level of theory with ECP, the conversion from a linear type isomer to a ring type isomer and vice versa was not observed during the simulation.

5. Results of the Simulation

5.A. Average Structure. To find the average structure at finite temperatures from the simulation, several angular and radial distribution functions for both linear and ring types of structures were analyzed. For the linear type of structures (see Figure 1), we are interested in the deviation from linearity. The angular distribution functions of the Si−C−C angle are shown in Figure 3 at 100, 200, and 300 K. The maximum of the peak is at 177° at 100 K, and it shifts to 174° at 200 K. At 300 K, the distribution is broader and covers the angle between 165° and 175°. Thus, the average structure of the linear type isomer has small bending of the Si−C−C angles. Examination of the distribution functions of the C−C and Si−Si distances show that at 100 K the maxima of the distributions of C−C distance (1.30 Å) and Si−Si distance (4.66 Å) are only slightly different from the C−C distance (1.31 Å) and Si−Si distance (4.79 Å) of the optimized structure with ROHF MP2/6-31+G*. Thus, in the average structure, the C−C and Si−Si distances are fluctuating around the optimized values. In the nonlinear geometry, the $^1\Delta$ state splits into $^1A'$ and $^1A''$ states, and hence four roots (one triplet from $^3\Sigma_g^-$, two singlets coming from the $_1\Delta$ state, and one singlet coming from the $^1\Sigma_g^+$ state) of the (4,3) CI should be of importance for assignment of the spectrum. However, examination of the roots shows that the fourth root is high in energy, and so the lowest three roots need to be taken into account for assigning the spectrum.

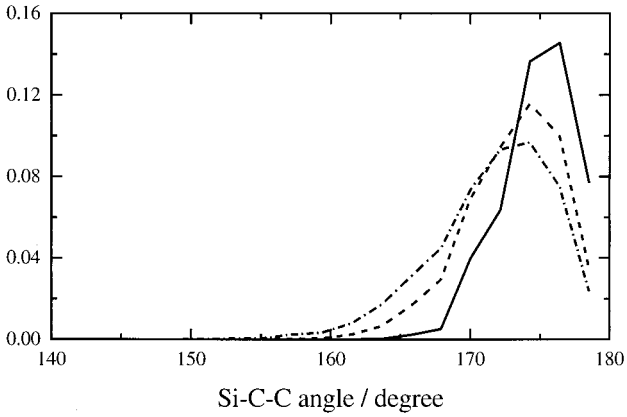

Figure 3. Angular distribution functions at 100, 200, and 300 K for the Si−C−C angle for the linear type of structures. Solid curve denotes the distribution at 100 K, dashed curve denotes the distribution at 200 K, and dash−dotted curve denotes the distribution at 300 K.

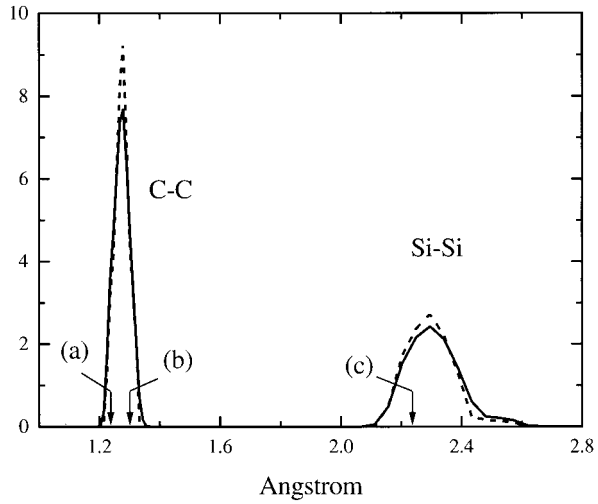

Figure 4. Radial distribution functions at 100 and 300 K of C−C and Si−Si distances for the ring type of structures. Dashed curves correspond to 100 K, and the solid curves correspond to 300 K. Arrows a and b denote the C−C distances in acetylene and ethylene. Arrow c denote the Si−Si distance in Si_2 molecule.

In ring isomers, even the backbone structure is floppy; the harmonic bending frequency of the Si(4)−C(1)-C(2) unit is as low as 336 cm^{-1}. The examination of the angular distribution function confirms the floppyness. Various radial distribution functions of the ring type were examined to find the average structure. At first, the Si−Si distance and C−C distance were examined and are shown at 100 and 300 K in Figure 4. It is seen from the figure that the maximum of the peak for Si−Si is at 2.3 Å, which is 0.1 Å smaller than the Si−Si distance of the optimized ring structure at the MP2 level with 6-31+G* basis set. This bond length suggests that the Si−Si bond is weaker than that of the Si_2 molecule[19] (See arrow c in Figure 4). The distribution has a shoulder from 2.4 to 2.6 Å. The distribution at 300 K has similar feature as the 100 K one, with slight broadening due to thermal fluctuation. It is also seen from the figure that the maximum of the peak for the C−C distance is at 1.28 Å, which is 0.05 Å shorter than that of the optimized structure. This bond length suggests that the C−C bond is stronger than the C−C bond of ethylene ((b) in Figure 4) but weaker than that of acetylene ((a) in Figure 4). The distribution at 300 K is slightly broader than that at 100 K. The Si−Si

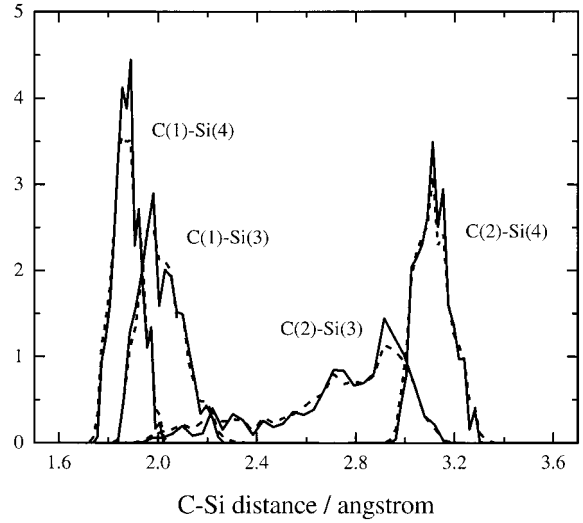

Figure 5. Radial distribution functions of C(1)−Si(3), C(1)−Si(4), C(2)−Si(3), and C(2)−Si(4) (see Figure 1 for atom numbering) distances at 100 and 300 K. Solid curves correspond to 100 K and dashed curves correspond to 300 K.

distribution is found to be broader than the C−C one. The above observation implies that the Si−Si and C−C distances in the average structure do not change much from those of the optimized one, which in turn implies that, in the average structure, both Si−Si and C−C distances are fluctuating around the values in the optimized structure.

To characterize the nature of the average structure of the ring isomer, four pairs of C−Si distribution functions were evaluated and are shown in Figure 5 at 100 and 300 K. We have found out the strongly and weakly bonded C−Si atoms from C(1)−Si(3) and C(1)−Si(4) distances at every sampled point of the simulation. It is seen from Figure 5 that the maximum of the C(1)−Si(4) distribution is around 1.83 Å, which should be compared with the 1.854 Å in the optimized structure. The distribution has a width of 0.2 Å and is not very sensitive to temperature. The C(1)−Si(3) distribution function shows that the maximum is at 1.99 Å (compare with 1.91 Å in the optimized structure). The distribution has a 0.4 Å width and again is not very sensitive to temperature. The C(2)−Si(4) distribution has the maximum at 3.1 Å (3.09 Å in the optimized structure). Combining the above observations, we can conclude that the average structure has a backbone of C(2)−C(1)−Si(4) and a rather rigid triangle of C(1)−Si(3)−Si(4) similar to the optimized structure. On the other hand, C(2)−Si(3) distribution is very different from the optimized structure (1.97 Å). It is extremely broad with a range from 1.9 to 3.2 Å. The distribution of the dihedral angle between the planes Si(4)−C(1)−C(2) and Si(4)−Si(3)−C(2) has two peaks close to 0° and 180°. In other words, the atom Si(3) is at both sides of the C(2)−C(1)−Si(4) backbone. Actually, it was found that the structure with Si(3) at the other side of the Si(4)−C(1)−C(2) backbone is the minimum at the 3-21G* level with ECP. Thus, in the average structure, there is out-of-plane movement of the Si(3) atom over the Si(4)−C(1)−C(2) plane. It is interesting to note that two carbons are not symmetric in the radial distribution, which implies that the barrier for the interchange of Si(4) and Si(3) is high. This was confirmed by determining the transition state, which is 1.33 eV above the energy of the ring isomer at the MP2/6-31+G* level. Thus, the average structure of the ring isomer has C(2)−C(1)−Si(4) bond with a mobile Si(3). The odd electron resides on C(2) and Si(4), so the C(2)−C(1)-Si(4) backbone is similar to the allene anion.

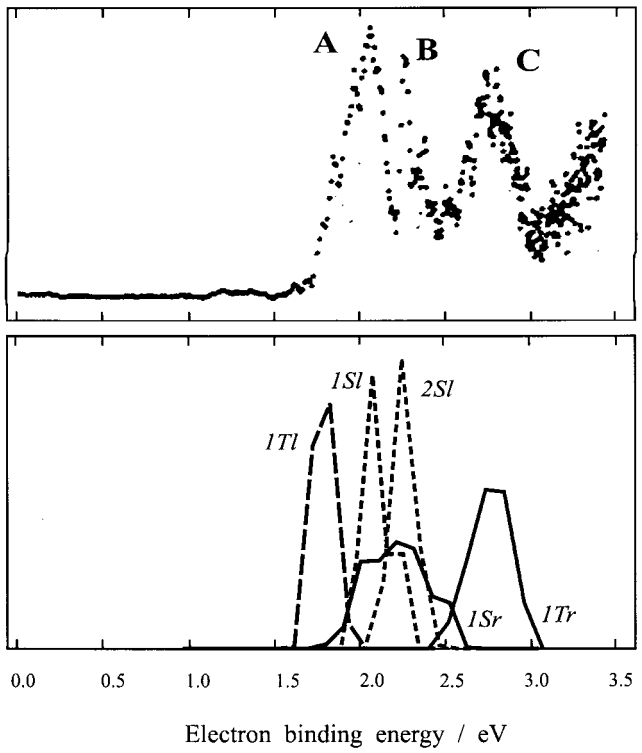

Figure 6. Calibrated (see text) vertical detachment energy (VDE) spectrum obtained from the simulation (shown at the bottom). The solid lines represent the simulated bands coming from the ring type of structures and dotted lines represent the simulated bands coming from the linear type of structures. For the labels 1Tl, 1Sl, etc., see text. The experimental spectrum is shown at the top for comparison

5.B. Assignment of the Spectrum from the Simulation. In Table 2, the differences in energy between the doublet anion and neutral (singlet and triplet) in the (4,3) CI and MRCI calculations are shown for both the ring and linear isomers. It is seen from the table that for the linear isomer, the singlet−triplet splittings are almost equal in the two calculations, whereas, for the ring structure, the difference is overestimated by 0.21 eV in the (4,3) CI calculation.

For comparison with the experimental spectrum, it is necessary to calibrate the simulated spectrum. In the present study, we use more reliable MRCI energy for calibration. The energy difference (see Table 2), which needs to be added to the VDEs calculated in the simulation, was taken as 0.61 eV for both singlet and triplet of the linear and 0.55 and 0.35 eV for singlet and triplet of the ring isomer, respectively. It is to be noted that even the MRCI calculation underestimates the VDEs by 0.1−0.3 eV (see discussion in section 3).

The experimental and simulated spectra are shown in Figure 6. Label 1Tl in the figure represents the band coming from the triplet state of the linear isomer, whereas labels 1Sl and 2Sl represent the first and second singlet states of the linear isomer. Similarly, 1Tr and 1Sr represent triplet and singlet states of the ring isomers, respectively. The bands due to ring type structures are much broader than those from linear type structures. It results from the flatness of the potential energy surface and is consistent with large fluctuation in the average structure obtained in the last section. The simulated spectrum is not smooth, probably because the number of points sampled in the simulation was not enough.

As is seen in Figure 6, the experimental band C around 2.6 eV and the simulated band 1Tr have almost the same position and feature. Evidently, band C is due to the triplet state of the

ring isomer. Band 1Sr acts as a background from 1.9 to 2.5 eV. The assignments of the other bands are less straightforward. But it is clear that the spectrum cannot be attributed to the ring isomer only. Also, it is true that three bands of the linear type isomers cannot explain the observed spectrum, particularly band C.

For the linear type of structures, bands 1Tl, 1Sl, and 2Sl have considerable overlap among them. The lowest band A in the experimental spectrum peaks at 2.0 eV, and has a shoulder at the low-energy side. The shape of band A suggests that it consists of at least two transitions. Because of the state ordering in the neutral linear isomer, it is most probable that the shoulder of A is the transition to the state originating from the linear triplet state (note that our calibrated energy tends to underestimate the detachment energy). The main strong peak of A is now assigned to the lowest singlet state (1Sl) of the linear type structure. The higher energy side of the sharp band B shows a little noisy structure. The observed peak B nearly coincides with the band 2Sl. The noise comes from the background band. Closer examination of the CI coefficients of the two singlet roots reveals that both of the states are produced by detachment of one electron without any rearrangement of the remaining electrons. Thus, both the bands are expected to contribute equally to the spectrum.

It is worth noting that the band due to the triplet state of the linear isomer is a little broader than those of the singlet states of the linear one. To understand it clearly, the energy distribution of the anionic state and the triplet and singlet states were examined. It was found that the triplet state has broader energy distribution than both the anion and singlet states, which implies the potential energy surface of the triplet state is steeper than those of the anion and singlet at our level of calculation.

Thus, both linear and ring isomers contribute to the observed photoelectron spectrum. We emphasize that the major result from the simulation is the broadness of the bands from the ring structure. This reflects a large nuclear motion at finite temperature of the clusters.

6. Conclusion

In the present work, structure and complex photoelectron spectrum of $Si_2C_2^-$ were investigated by MRCI calculation and by a combination of CI calculation and multicanonical Monte Carlo simulation. In the first step of the investigation, structures of $Si_2C_2^-$ were optimized at the MP2/6-31+G* level of theory. We found two structures which are at the minima of the potential energy surface, linear and ring. In the next step, MRCI calculation reveals that there are two photodetached states ($^1A'$, $^3A''$) for the ring isomer and three states ($^1\Delta_g$, $^1\Sigma_g^+$, and $^3\Sigma_g^-$) for the linear isomer, which might contribute to the spectrum. Finite temperature effects on the spectrum and structure were taken into account by performing multicanonical Monte Carlo simulation with small CI calculation at each step of the simulation. It was found that for the linear isomer, average structure at 100 K, has less than 5° bending of the Si−C−C angle, whereas for the ring isomer the average structure consists of Si−C−C backbone and the other silicon has an out-of-plane movement. Simulated spectra were compared with the experimental one. The peak at 2.6 eV corresponds to the transition to the ring isomer, and the main contribution to the peak at the 2.0 eV comes from the triplet and singlet state for the linear isomer. The peak at 2.2 eV has contributions from another singlet linear state. The broad band due to the singlet state of the ring isomer acts as a background band from 2.0 to 2.5 eV. The effect of finite temperature on the spectrum was manifested in the broad bands due to the ring structure.

Thus, the highly complex photoelectron spectrum of $Si_2C_2^-$ was assigned from first principles by including the movement of the nuclei. Multicanonical simulation with ab initio MO calculation was found to be a robust technique for explaining complex molecular phenomena. We intend to use the same technique for elucidating photoelectron and electronic spectra of clusters and large molecules.

Acknowledgment. This work was partially supported by the Grants-in-Aid for Scientific Research (A) (no. 09304057) of Ministry of Education, Science, Sports and Culture of Japan. One of the authors (P.B.) is a recipient of a foreign student scholarship from the Ministry of Education, Science, Sports and Culture of Japan.

References and Notes

(1) Bertolus, M.; Brenner, V.; Millie, P. *Eur. Phys. J. D* **1998**, *1*, 197.
(2) Hunsicker, S.; Jones, R. O. *J. Chem. Phys.* **1996**, *105*, 5048.
(3) Nakajima, A.; Taguwa, T.; Nakao, K.; Gomei, M.; Kishi, R.; Iwata, S.; Kaya, K. *J. Chem. Phys*. **1995**, *103*, 2050.
(4) Presilla-marquez, J. D.; Rittby, C. M. L.; Graham, W. R. M. *J. Chem. Phys.* **1997**, *106*, 8367.
(5) Raghavachari, K.; Binkley, J. S. *J. Chem. Phys.* **1987**, *87*, 2191.
(6) Andreoni, W.; Pastore, G. *Phys. Rev. B* **1990**, *41*, 10243.
(7) Kishi, R.; Gomei, M.; Nakajima, A.; Iwata, S.; Kaya, K. *J. Chem. Phys.* **1996**, *104*, 8593.
(8) Gomei, M.; Kishi, R.; Nakajima, A.; Iwata, S.; Kaya, K. *J. Chem. Phys.* **1997**, *107*, 10051.
(9) Werner, H. J.; Knowles, P. J. *J. Chem. Phys.* **1988**, *89*, 5803.
(10) Molpro is a package of ab initio programs written by Werner, H. J. and Knowles, P. J., with contributions from Almlof, J.; Amos, R. D.; Berning, A.; Deegan, J. O.; Eckert, F.; Elbert, S. T.; Hampel, C.; Lindh., R.; Meyer, W.; Nicklass, A.; Peterson, K.; Pitzer, R.; Stone, A. J.; Taylor, P. R.; Mura, M. E.; Pulay, P.; Schuetz, M.; Stoll, H.; Thorsteinsson, T.; Cooper, D. L.
(11) Schmidt, M. W.; Baldridge, K. K.; Boatz, J. A.; Elbert, S. T.; Gordon, M. S.; Jensen, J. H.; Koseki, S.; Matsunaga, N.; Nguyen, K. A.; Su, S. J.; Windus, T. L.; Dupuis, M.; Montgomery, J. A. *J. Comput. Chem.* **1988**, *14*, 158.
(12) Frisch, M. J.; Trucks, G. W.; Schlegel, H. B.; Gill, P. M. W.; Johnson, B. G.; Robb, M. A.; Cheeseman, J. R.; Keith, T.; Peterson, G. A.; Montogomery, J. A.; Raghavachari, K.; Al-laham, M. A.; Zakrzewski, V. G.; Ortiz, J. V.; Foresman, J. B.; Cioslowski, J.; Stefanov, B. B.; Nanayakkra, A.; Challacombe, M.; Peng, C. Y.; Ayala, P. Y.; Chen, W.; Wong, M. W.; Andres, J. L.; Replogle, E. S.; Gomperts, R.; Martin, R. L.; Fox, D. J.; Binkley, J. S.; Defress, D. J.; Baker, J.; Stewart, J. P.; Headgordon, M.; Gonzalez, C.; Pople, J. A. *Gaussian94*, revision C.3; Gaussian Inc.: Pittsburgh, PA, 1995.
(13) Dunning, T. H. *J. Chem. Phys.* **1989**, *90*, 1007.
(14) Fitzgerald, G. B.; Barlett, R. J. *Int. J. Quantum. Chem.* **1990**, *38*, 121.
(15) Bandyopadhyay, P.; Ten-no, S.; Iwata. S. *Mol. Phys.* **1999**, *96*, 349.
(16) Berg, B. A.; Neuhaus, T. *Phys. Lett. B* **1991**, *267*, 249.
(17) Ferrenberg, A. M.; Swendsen, R. H. *Phys. Rev. Lett.* **1988**, *61*, 2635; **1989**, *63*, 1658(E) and references given in the erratum.
(18) Stevens, W. J.; Basch, H.; Krauss. M. *J. Chem. Phys* **1984**. *81*, 6026.
(19) Raghavachari, K.; Logovinsky, V. *Phys. Rev. Lett.* **1985**, *55*, 2853.